Biomedicine & Pharmacotherapy 153 (2022) 113419

Contents lists available at ScienceDirect

Biomedicine & Pharmacotherapy

journal homepage: www.elsevier.com/locate/biopha

Short communication

Antagonism of miR-148a attenuates atherosclerosis progression in *APOB*^{TG}*Apobec*$^{-/-}$*Ldlr*$^{+/-}$ mice: A brief report

Noemi Rotllan [a,b,c,d,*], Xinbo Zhang [a,b], Alberto Canfrán-Duque [a,b], Leigh Goedeke [a,b], Raquel Griñán [c,e], Cristina M. Ramírez [b,f], Yajaira Suárez [a,b], Carlos Fernández-Hernando [a,b]

[a] Vascular Biology and Therapeutics Program, Yale University School of Medicine, New Haven, CT, USA
[b] Integrative Cell Signaling and Neurobiology of Metabolism Program, Department of Comparative Medicine and Department of Pathology, Yale University School of Medicine, New Haven, CT, USA
[c] Institut d'Investigació Biomèdica Sant Pau (IIB SANT PAU), Barcelona, Spain
[d] CIBER de Diabetes y Enfermedades Metabólicas Asociadas (CIBERDEM), Barcelona, Spain
[e] Departament de Bioquímica i Biologia Molecular, Universitat Autònoma De Barcelona, Barcelona, Spain
[f] IMDEA Research Institute of Food and Health Sciences, Madrid, Spain

ARTICLE INFO

Keywords:
MiR-148a
Atherosclerosis progression
Therapeutic inhibition
Plaque stability
Cholesterol Efflux
M2-like phenotype

ABSTRACT

Objective: miR-148a-3p (miR-148a) is a hepatic and immune-enriched microRNA (miRNA) that regulates macrophage-related lipoprotein metabolism, cholesterol homeostasis, and inflammation. The contribution of miR-148a-3p to the progression of atherosclerosis is unknown. In this study, we determined whether miR-148a silencing mitigated atherogenesis in *APOB*^{TG}*Apobec*$^{-/-}$*Ldlr*$^{+/-}$ mice.

Methods: *APOB*^{TG}*Apobec*$^{-/-}$*Ldlr*$^{+/-}$ mice were fed a typical Western-style diet for 22 weeks and injected with a nontargeting locked nucleic acid (LNA; LNA control) or miR-148a LNA (LNA 148a) for the last 10 weeks. At the end of the treatment, the mice were sacrificed, and circulating lipids, hepatic gene expression, and atherosclerotic lesions were analyzed.

Results: Examination of atherosclerotic lesions revealed a significant reduction in plaque size, with marked remodeling of the lesions toward a more stable phenotype. Mechanistically, miR-148a levels influenced macrophage cholesterol efflux and the inflammatory response. Suppression of miR-148a in murine primary macrophages decreased mRNA levels of proinflammatory M1-like markers (*Nos2*, *Il6*, *Cox2,* and *Tnf*) and increased the expression of anti-inflammatory genes (*Arg1*, *Retlna,* and *Mrc1*).

Conclusions: Therapeutic silencing of miR148a mitigated the progression of atherosclerosis and promoted plaque stability. The antiatherogenic effect of miR-148a antisense therapy is likely mediated by the anti-inflammatory effects observed in macrophages treated with miR-148 LNA and independent of significant changes in circulating low-density lipoprotein cholesterol (LDL-C) and high-density lipoprotein cholesterol (HDL-C).

1. Introduction

Many recent studies have demonstrated that microRNAs (miRNAs) play key roles in the control of mRNA translation and degradation in nearly all biological processes [1–4]. Thus, they represent a level of posttranscriptional regulation not previously recognized. As dysregulation of miRNAs is involved in the development of many diseases, targeting miRNAs is a promising therapeutic approach [5–9].

Alterations in the control of cholesterol homeostasis can lead to pathological processes, including atherosclerosis, the most common

Abbreviations: ABCA1, ATP binding cassette A-1; APOA1, apolipoprotein A-1; APOB, apolipoprotein B; ARG1, arginase 1; BMDM, bone marrow-derived macrophage; CI, control inhibitor; CM, control mimic; COX2, cyclooxygenase 2; FPLC, fast protein liquid chromatography; FBS, fetal bovine serum; H&E, hematoxylin and eosin; HDL-C, high-density lipoprotein cholesterol; Inh-148a, miR-148a inhibitor; INF-γ, interferon gamma; LDL-C, low-density lipoprotein cholesterol; LDLR, low-density lipoprotein receptor; LNA, locked nucleic acid; miRNA, microRNA; LPS, lipopolysaccharide; ORO, Oil-Red O; RETLNA, resistin like alpha; TNF-α, tumor necrosis factor alpha; PBS, phosphate buffered saline; SDS-PAGE, sodium dodecyl sulfate−polyacrylamide gel electrophoresis; αSMA, smooth muscle alpha-actin; qRT-PCR;, quantitative real-time polymerase chain reaction; WT, wild type.

* Corresponding author at: Institut d'Investigació Biomèdica Sant Pau (IIB SANT PAU), Barcelona, Spain.
E-mail address: NRotllanV@santpau.cat (N. Rotllan).

https://doi.org/10.1016/j.biopha.2022.113419
Received 26 January 2022; Received in revised form 12 July 2022; Accepted 13 July 2022
Available online 19 July 2022

cause of mortality in Western societies [10–13]. High levels of low-density lipoprotein cholesterol (LDL-C) and low levels of high-density lipoprotein cholesterol (HDL-C) are associated with increased cardiovascular disease risk [13–15]. In humans, most serum cholesterol is transported as cholesterol esters in LDL particles. The uptake of LDL and other ApoE/ApoB-containing lipoproteins occurs through low-density lipoprotein receptor (LDLR) and is a classic example of receptor-mediated endocytosis [16,17]. Maintenance of cellular cholesterol homeostasis requires constant metabolic adjustment, which is achieved partly by fine-tuned regulation of classical transcription factors (e.g., sterol regulatory element-binding protein 2 and liver X receptor) and partly by members of a class of small non-coding RNAs, termed miRNAs [18–21]. miRNAs are critical components of the cholesterol regulatory circuitry, and many miRNAs (miR-122, miR-30c, miR-33, miR-758, miR-106b, miR-144, and miR-223) have been shown to control lipid metabolism in vivo [22–34]. We and others have previously demonstrated that miR-148a negatively regulates the expression and activity of LDLRs [35–37]. Research has also shown that inhibition of hepatic miR-148a in hypercholesterolemic mice by antisense oligonucleotides increases LDLR expression and decreases circulating LDL-C [35–37]. These results correlate with those of two independent genome-wide association studies showing a single nucleotide polymorphism in the miR-148a locus associated with altered blood LDL-C [38,39]. miR-148a has also been shown to suppress the expression of ATP binding cassette A-1 (ABCA1), a transporter that controls HDL generation and cellular cholesterol efflux [37].

In addition to the regulation of circulating cholesterol, miR-148a regulates cholesterol efflux and inflammation [40,41]. MiR-148a is highly expressed in macrophages, and miR-148a overexpression promotes macrophage proinflammatory M1 polarization [40,41]. Moreover, miR-148a controls cell proliferation, differentiation, and growth, as well as immune responses, by suppressing the expression of proinflammatory molecules, such as interleukin-12, interleukin-6, tumor necrosis factor alpha (TNF-α), and interferon gamma (INF-γ) [42,43]. In addition to its prominent role in regulating macrophage cholesterol metabolism and the inflammatory response, a recent study pointed to a regulatory role for miR-148a in atherosclerosis, with this study finding that miR-148a levels were selectively upregulated in patients with atherosclerosis [44]. Based on these findings, we hypothesized that antagonism of miR-148a might attenuate the progression of atherosclerosis by decreasing circulating LDL-C, increasing plasma HDL-C levels, promoting macrophage cholesterol efflux, and attenuating the macrophage proinflammatory response. To test this hypothesis, we silenced miR-148a in *APOB*^{TG}*Apobec*$^{-/-}$*Ldlr*$^{+/-}$ mice, which synthesize hepatic ApoB-100-containing lipoproteins (VLDL and LDL) and have one functional allele for the *Ldlr* gene, allowing clearance of circulating LDL by LDLRs. Our results showed that therapeutic targeting of miR-148a using a locked nucleic acid (LNA) significantly attenuated atherogenesis and reduced vascular inflammation. This atheroprotection observed in mice treated with miR-148a inhibitors was likely mediated by increasing cholesterol efflux and polarization to an M2-like phenotype in atherosclerotic macrophages rather than affecting circulating lipoproteins.

2. Materials and methods

The data, analytical methods, and study materials that support the findings of this study are available to other researchers upon reasonable request. Details on the research materials are provided online in Supplemental materials.

2.1. Animals and LNA 148a treatment

APOB$^{TG-/-}$*Ldlr*$^{+/-}$ mice were kindly provided by Dr. Daniel Rader. Male *APOB*^{TG}*Apobec*$^{-/-}$*Ldlr*$^{+/-}$ mice were generated by breeding with *Apobec*$^{-/-}$ mice. The animals were kept under constant temperature and humidity in a 12-hour controlled dark/light cycle. Accelerated atherosclerosis was induced by feeding mice a high-cholesterol diet containing 1.25 % cholesterol (D12108; Research Diets, Incorporated, New Brunswick, NJ, USA) for 12 weeks. All the experiments were approved by the Institutional Animal Care Use Committee of Yale University School of Medicine.

For miR-148a inhibition experiments, 8-week-old male *APOB*^{TG} *Apobec*$^{-/-}$; *Ldlr*$^{+/-}$ mice were fed a high-cholesterol diet for 22 weeks and then randomized into two groups: LNA control ($n = 10$) and LNA 148a ($n = 10$). The mice received intraperitoneal injections of 5 mg/kg body weight LNA control (5′-ACGTCTATACGCCCA-3′) or LNA 148a (5′-TTCTGTAGTGCACTG-3′) oligonucleotides (Exiqon) every 3 days for 10 weeks. Twenty-four hours after the final injection, the mice were euthanized, and sera, livers, hearts, and aortas were taken for further analysis.

2.2. Lipoprotein profile and lipid measurements

The mice fasted for 12–16 h overnight before blood samples were collected by retro-orbital venous plexus puncture. Plasma was separated by centrifugation. HDL-C was isolated by precipitation of non-HDL-C, and both HDL-C fractions and total plasma were stored at − 80 °C. Total plasma cholesterol and triglycerides (TAGs) were enzymatically measured (Wako Pure Chemicals Tokyo, Japan) according to the manufacturer's instructions. The lipid distribution in plasma lipoprotein fractions was assessed by fast protein liquid chromatography (FPLC) gel filtration using 2 Superose 6 HR 10/30 columns (Pharmacia Biotech, Uppsala, Sweden). Cholesterol in each fraction was determined using the enzymatic method. Plasma alanine aminotransferase, aspartate aminotransferase, and albumin in the LNA control mice and mice treated with LNA 148a were analyzed by Yale University School of Medicine Mouse Metabolic Phenotype Center.

2.3. Histology, immunohistochemistry, and morphometric analyses

Murine hearts and livers were perfused with phosphate buffered saline (PBS) and placed in 10 ml of 4 % paraformaldehyde for 4 h. After incubation in paraformaldehyde, the hearts were washed with PBS, followed by immersion in PBS for 1 h and then 30 % sucrose overnight. Finally, the hearts and livers were embedded in OCT and frozen. Serial Section 6 μm thick were cut from the hearts using a cryostat. Every fourth slide from the serial sections was stained with hematoxylin and eosin (H&E) for quantification of the lesion area. In each mouse, aortic lesion size was obtained by averaging the lesion area in at least nine sections from the same animal. The fibrous cap and necrotic core area were measured as a percentage of the total plaque area. A necrotic core region was defined as a clear area that was H&E free [45]. Boundary lines were drawn around these regions, and the area measurements were obtained by image analysis software (see below). Fibrous cap thickness was determined by selecting the largest necrotic core from triplicate sections and taking a measurement from the thinnest part of the cap, determined by measuring the area between the outer edge of the cap and necrotic core boundary [45]. CD68 and smooth muscle alpha-actin (αSMA) staining were used as macrophage and vascular smooth muscle cell markers, respectively, using consecutive slides from serial sections. Nuclei were counterstained with DAPI. Serial sections 8 μm thick were cut from livers using a cryostat. Every third slide from the serial section was stained with H&E, and each consecutive slide was stained with Oil-Red O (ORO) for visualization of neutral lipids as previously described [46]. NIH ImageJ software (National Institutes of Health, Bethesda, MD, USA) was used for all quantifications.

2.4. En face ORO staining

ORO stock solution (35 ml, 0.2 % weight/volume in methanol) was mixed with 10 ml of 1 M NaOH and filtered. Aortas were opened up

longitudinally and briefly rinsed with 78 % methanol, stained with 0.16 % ORO Solution for 50 min, and then destained in 78 % methanol for 5 min. The lesion area was quantified as a percent of the ORO staining area in the total aorta area.

2.5. Cell culture

Peritoneal macrophages from wild-type (WT) mice were harvested by peritoneal lavage 4 days after an intraperitoneal injection of thioglycollate (3 % w/v). The cells were plated in RPMI 1640 medium supplemented with 10 % fetal bovine serum (FBS), 100 U/ml of penicillin, and 100 U/ml of streptomycin. After 4 h, nonadherent cells were washed out, and the macrophages were incubated in fresh medium containing DMEM, 20 % FBS, and 20 % L-cell–conditioned medium for 2 days. The cells were maintained in culture as an adherent monolayer by adding fresh medium every day. The peritoneal macrophages were used for different experiments. Bone marrow-derived macrophages (BMDMs) from adult male WT mice were harvested and cultured in Iscove's modified Dulbecco's medium supplemented with 20 % FBS and 20 % L-cell conditioned medium. After 7 days in culture, nonadherent cells were eliminated, and adherent cells were harvested for the assay. The BMDMs were then used for polarization experiments.

2.6. Transfection with an miRNA mimic or an inhibitor

The BMDMs or thioglycollate-elicited peritoneal macrophages were seeded at a density of 1×10^6 cells per well. They were then transfected for 48 h with a control mimic (CM, 40 nM), miR-148a mimic (miR-148a), control inhibitor (CI, 60 nM), or miR-148a inhibitor (Inh-148a) (Dharmacon) utilizing RNAimax (Invitrogen), following the manufacturers' standard protocols.

2.7. M1 and M2 polarization assay

The BMDMs from WT mice were transfected with the CM and miR-148a or CI and Inh-148a for 48 h. They were then stimulated for the last 8 h with interleukin-4 (15 ng/ml; R&D) or LPS (10 ng/ml; Sigma-Aldrich) and INF-γ (20 ng/ml; R&D) to polarize macrophages to M2 or M1, respectively. At the end of the treatment, the cells were extensively washed with 1 × PBS, and RNA was isolated.

2.8. Cholesterol efflux assays

Cholesterol efflux assays were performed as previously described [47]. Briefly, the thioglycollate-elicited peritoneal macrophages were seeded at a density of 8×10^5 cells per well and transfected with either a CM or miR-148a mimic (miR-148a). Following 48 h of transfection, the cells were loaded with 0.5 μCi/ml of ^{3}H-cholesterol for 24 h. Twelve hours after loading, the cells were incubated with 3 μM T090 to increase the expression of ABCA1. The cells were then washed twice with PBS and incubated in DMEM supplemented with 2 mg/ml of fatty-acid free bovine serum albumin medium in the presence of an ACAT inhibitor (2 μmol/L) for 4 h prior to the addition of 50 μg/ml of human apolipoprotein A-1 (ApoA1) in fatty-acid free bovine serum albumin medium, with or without the indicated treatments. Supernatants were collected 6 h later, and efflux was expressed as a percentage of the total cell ^{3}H-cholesterol content (total effluxed ^{3}H-cholesterol + cell-associated ^{3}H-cholesterol).

2.9. Western blot analysis

Liver tissue was homogenized using a Bullet Blender. The tissue was lysed in ice-cold buffer containing 50 mM Tris–HCl, pH 7.5, 0.1 % sodium dodecyl sulfate (SDS), 0.1 % deoxycholic acid, 0.1 mM EDTA, 0.1 mM EGTA, 1 % NP-40, 5.3 mM NaF, 1.5 mM NaP, 1 mM orthovanadate, 1 mg/ml of protease inhibitor cocktail (Roche), and 0.25 mg/ml of AEBSF (Roche). Lysates were sonicated and rotated at 4 °C for 1 h. Insoluble material was then removed by centrifugation at 12,000 × *g* for 10 min. After normalizing of the total protein amount, the cell lysates were resuspended in SDS sample buffer before separation by SDS–polyacrylamide gel electrophoresis (SDS–PAGE). Following transfer of the proteins onto nitrocellulose membranes, the membranes were probed with the following antibodies: mouse monoclonal antibodies against ABCA1 (#18180; 1:1000; Abcam) and apolipoprotein A-1 (APOA1) (#ab20453; 1:1000; Abam); rabbit polyclonal antibody against LDLR (#1007665; 1:1000; Cayman Chemical); mouse monoclonal antibody against APOB (#K23300R; 1:2000; Meridian Life Science), and a mouse monoclonal antibody against HSP90 (#610419; 1:1000; BD Bioscience). Protein bands were visualized using the Odyssey Infrared Imaging System (LI-COR Biotechnology), and densitometry was performed using ImageJ software from NIH (http:/rsbweb.nih.gov/ij/).

For western blot analysis of APOB and APOA1 in lipoprotein fractions, an equal volume of three fractions was mixed with reducing SDS sample buffer and separated on a NuPAGE Novex 4–12 % Tris-Acetate Mini Gel using 1x NuPAGE Tris-acetate SDS running buffer (Invitrogen). Following overnight transfer of proteins onto nitrocellulose membranes, the membranes were blocked in 5 % (wt/vol) nonfat milk dissolved in wash buffer. The membranes were then probed with an antibody against APOB and APOA1 overnight at 4ºC, washed, incubated with fluorescently labeled secondary antibodies, and visualized as described previously.

2.10. RNA isolation and quantitative real-time polymerase chain reaction (qRT-PCR)

Total RNA from liver tissue was isolated using TRIzol reagent (Invitrogen) according to the manufacturer's protocol. For mRNA expression analysis, cDNA was synthesized using iScript RT Supermix (Bio-Rad), following the manufacturer's protocol. qRT-PCR analysis was performed in duplicate using SsoFast EvaGreen Supermix (BioRad) on an iCycler Real-Time Detection System (Eppendorf). The mRNA levels were normalized to 18 S. For miRNA quantification, Taqman mature miRNA detection kits were used. Primers specific for human miR-148a were used for cDNA production and qRT-PCR analysis and normalized to U6 as a housekeeping gene. miR-148a quantification and qRT-PCR were performed in duplicate using Taqman RT mix on an iCycler Real-Time Detection System (Eppendorf).

2.11. Analysis of circulating leukocytes

Blood was collected by retro-orbital puncture in heparinized microhematocrit capillary tubes. Total circulating numbers of blood leukocytes were measured using a HEMAVET system. For further FACs analysis, erythrocytes were lysed with ACK lysis buffer (155 mN ammonium chloride, 10 nM potassium bicarbonate, and 0.001 mM EDTA, pH 7.4). White blood cells were resuspended in 3 % FBS in PBS, blocked with 2 mg/ml of FcgRII7III, then stained with a cocktail of antibodies. For monocyte identification, the following antibodies were used: FITC-Ly6-C (AL-21), PE-CD115 (AFS98), and APC-Ly6-G (1A8) (all from BioLegend, San Diego, CA, USA). CD115^{hi} monocytes and subsets as Ly6-C^{hi} and Ly6-C^{lo} monocytes were identified.

2.12. Statistical analysis

The sample size in each experiment was selected based on similar studies in the literature. Details on the number of animals in each experiment are provided in the figures. In vitro experiments were routinely repeated at least three times, unless otherwise noted. Data are presented as mean ± standard error of the mean (SEM). Statistical differences were measured using an unpaired two-sided Student's *t*-test and a one-way analysis of variance with Bonferroni correction for multiple comparisons. Normality was checked using the Kolmogorov−Smirnov

test. A nonparametric test (Mann−Whitney) was used when data did not pass the normality test. Significance was accepted at the level of $p < 0.05$. The data analysis was performed using GraphPad Prism Software Version 8 (GraphPad, San Diego, CA, USA).

3. Results

To assess the effect of miR-148a silencing on the progression of atherosclerosis, male *APOB*^{TG}*Apobec*$^{-/-}$*Ldlr*$^{+/-}$ mice were injected every 3 days for 10 weeks with 5 mg per kg of body weight (mg/kg) of LNA antisense oligonucleotides targeting miR-148a (LNA 148a). A scrambled nontargeting LNA oligonucleotide was used as a control (LNA control). Twenty-four hours after the last injection, the mice were sacrificed, and sera and livers were collected for plasma lipid and gene expression analysis, respectively (Fig. 1A). To determine treatment efficacy, hepatic expression of miR-148a was measured in the mice injected with the LNA control and LNA 148a. Hepatic miR-148a levels were markedly reduced in the mice treated with LNA 148a compared to those treated with the LNA control (Fig. 1B). Hepatic expression of several miR-148 target genes, including *Abca1* and *Ldlr*, was increased in the mice treated with LNA 148a (Fig. 1C). No differences in body weight, glucose, or circulating leukocytes were found between the treatments (Figs. IA−C, Supplementary data [online]). In the LNA 148a group, total cholesterol levels were slightly decreased, whereas those of HDL-C were slightly

Figure 1

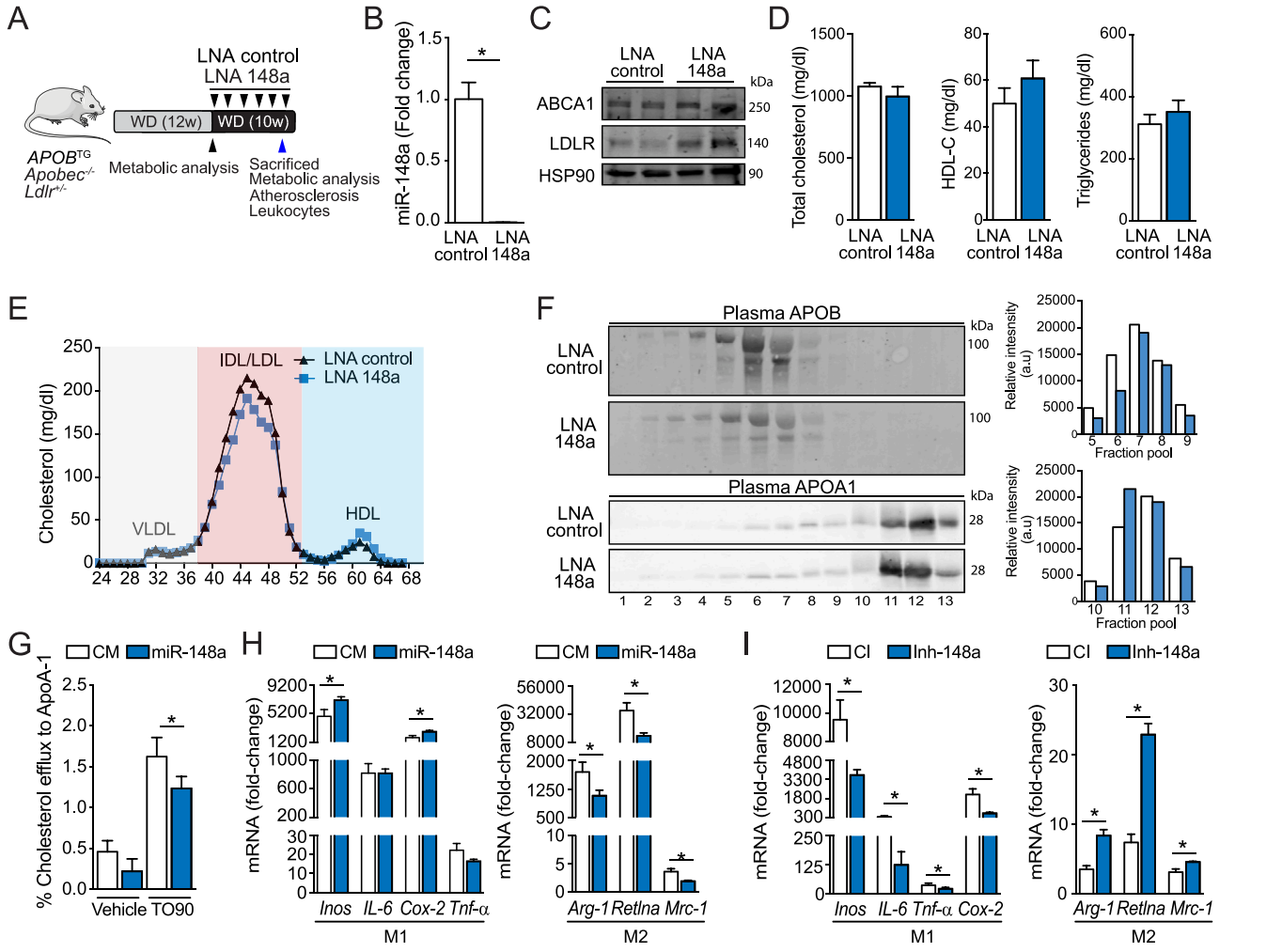

Fig. 1. Inhibition of miR-148a did not significantly alter plasma cholesterol levels in *APOB*^{TG}*Apobec*$^{-/-}$*Ldlr*$^{+/-}$ mice but promoted macrophage polarization toward an M2-like phenotype. (A) Experimental outline of LNA control or LNA 148a treated mice ($n = 9$ −10 per group). (B) qRT-PCR analysis of miR-148a from the livers of mice treated as in panel A. Data are the mean ± SEM. * $p < 0.05$ compared to the LNA control treatment group in an unpaired an *t*-test. (C) Representative Western blot analysis of ABCA1 and LDLR in livers of mice treated as in panel A. Relative protein levels were determined by band densitometry and were expressed in arbitrary units after correction for HSP90 (loading control). (D) Total cholesterol, HDL-C, LDL-C, and triglyceride levels in mice treated with the LNA control or LNA 148a. Data are shown as mean ± SEM ($n = 9$ −10 per group). (E) Lipoprotein profile analysis from pooled plasma ($n = 6$) obtained from mice treated with the LNA control or LNA 148a. (F) Western blot analysis (representative of two blots) of plasma APOB and APOA1 in FPLC-fractioned plasma lipoproteins in panel E. Lanes 1–13 correspond to the following pooled fractions: 1 (28−30), 2 (31−33), 3 (34−36), 4 (37−39), 5 (40−42), 6 (43−45), 7 (46−48), 8(49−51), 9 (52−54), 10 (55−57), 11 (58−60), 12 (61−63), and 13 (64−66). The relative intensities of APOB and APOA1 are shown on the right. (G) Cholesterol efflux to APOA1 in peritoneal macrophages isolated from WT mice stimulated with or without T0901317 (TO90) and transfected with a control (CM) or an miR-148a mimic (miR-148a). Data represent the mean ± SEM of duplicate samples ($n = 3$ per group). * $p < 0.05$, level of significance was determined using a *t*-test. (H) Gene expression of several M1 markers after transfecting bone marrow-derived monocytes for 48 h with a CM or miR-148a and stimulating them with LPS (10 ng/ml) and INF-γ (20 ng/ml) or M2 markers after incubating with interleukin-4 (15 ng/ml) for the last 8 h. (I) Similar to the experiment indicated in panel H but transfected with a CI or Inh-148a, mRNA expression levels were normalized to 18 S. Quantification represents the mean ± SEM ($n = 3$). Similar results were observed in three independent experiments. * $p < 0.05$ compared to the CM by an unpaired *t*-test.

increased, but the differences did not reach statistical significance (Fig. 1D). Plasma triglyceride levels were similar in both groups (Fig. 1D). We further characterized the effect of miR-148a silencing on circulating lipids by measuring the cholesterol content of different lipoproteins by FPLC (Fig. 1E). The results revealed a moderate decrease in plasma LDL-C levels and a slight increase in HDL-C levels in the mice treated with LNA miR-148a, which correlated with increased hepatic expression of LDLR and ABCA1, respectively. As expected, based on the decrease in LDL-C and increase in HDL-C fractions, the expression level of APOB100 was reduced, whereas that of APOA1 was increased in pooled plasma samples isolated from the mice treated with LNA 148a as compared to those treated with the LNA control (Fig. 1F). The effects of LNA 148a on lipoprotein metabolism did not affect liver toxicity, as indicated by similar levels of hepatic neutral lipid accumulation and circulating levels of alanine transaminase, asparagine transaminase, and albumin in the LNA 148a and LNA control treatment groups (Figs. ID–F, Supplementary data [online]).

Similar to the previous results of our study using J774 cells and BMDMs, overexpression of miR-148a in thioglycolate-elicited macrophages significantly attenuated cholesterol efflux to ApoA1 (Fig. 1G). In addition, macrophages transfected with miR-148a expressed higher levels of M1 markers (*Nos2* and *Cox2*) and lower levels of M2 markers (*Arg1*, *Retlna,* and *Mrc1*) (Fig. 1H). Conversely, inhibition of miR-148a polarized macrophages toward an M2 phenotype (Fig. 1I). Together,

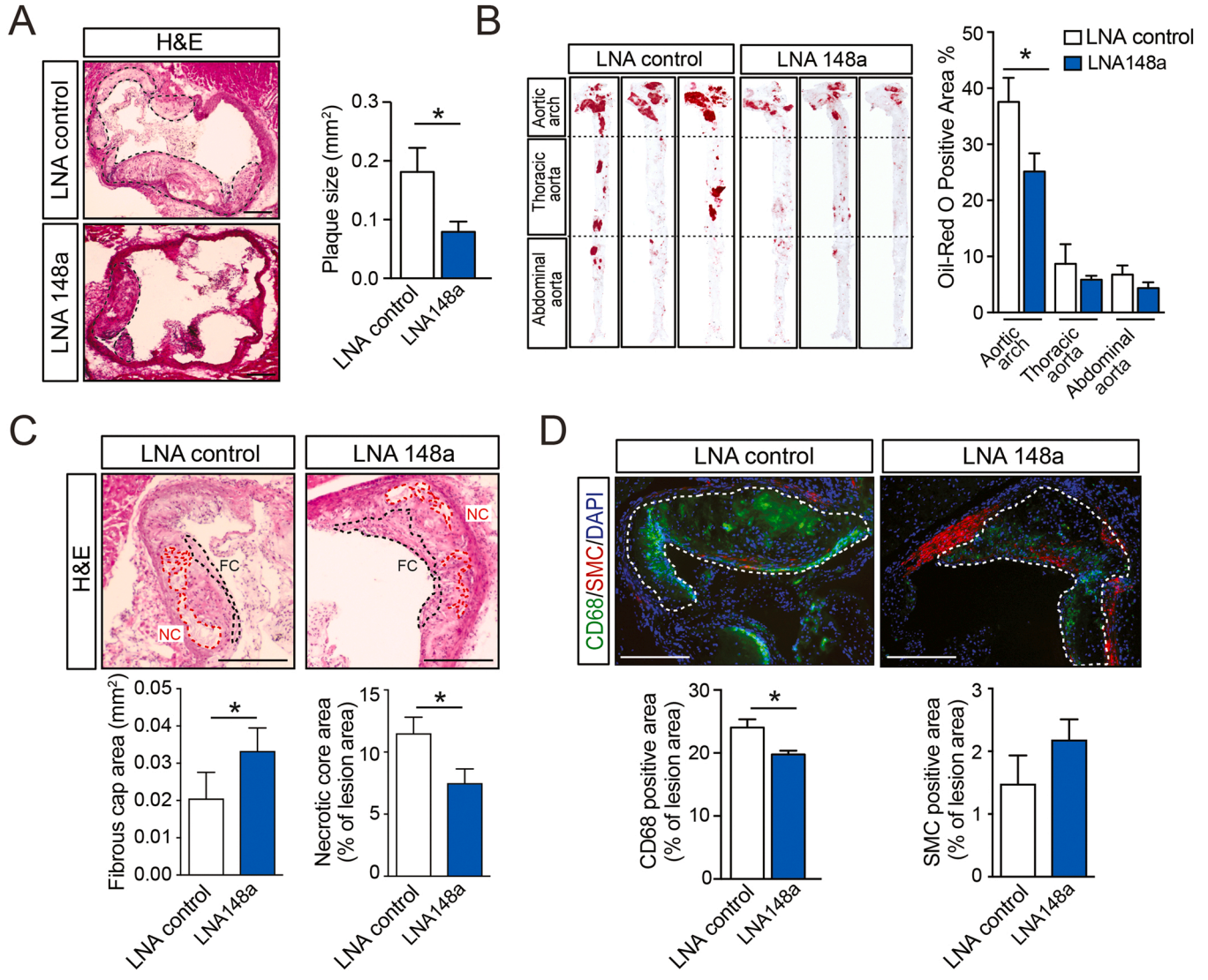

Fig. 2. Anti-miR-148a therapy mitigated atherosclerosis and promoted atherosclerotic plaque stability. (**A**) Representative histological analysis of cross sections of aortic sinus stained with H&E from *APOB*^{TG}*Apobec*$^{-/-}$*Ldlr*$^{+/-}$ mice treated with the LNA control or LNA 148a. The dashed lines show the boundary of the lesions. Quantification of plaque size is shown in the right panel. Data represent the mean ± SEM of plaque size quantified from nine sections from individual animals ($n = 9$ –10 per group); * $p < 0.05$, level of significance was determined using the Mann–Whitney test. Scale bars, 400 μm (**B**) Representative en face ORO staining of aortas from *APOB*^{TG}*Apobec*$^{-/-}$*Ldlr*$^{+/-}$ mice treated with LNA control or LNA 148a. Quantification of the ORO positive area is shown in the right panel and represents the mean ± S.E.M ($n = 9$ –10 per group). * $p < 0.05$, level of significance was determined using a one-way analysis of variance with Bonferroni's post-test. (**C**) Representative histological analysis of cross sections of aortic sinus stained with H&E from *APOB*^{TG}*Apobec*$^{-/-}$*Ldlr*$^{+/-}$ mice treated with the LNA control or LNA 148a. The black and red dashed lines show the boundary of the fibrous cap (FC) and necrotic core (NC), respectively. Quantification of the fibrous cap and necrotic core is shown in the bottom panel and represents the mean ± SEM of the quantification of nine sections from individual animals ($n = 9$ –10 per group); * $p < 0.05$, level of significance was determined using the Mann–Whitney test. Scale bars, 200 μm (**D**) Representative immunofluorescence analysis of macrophages (CD68; green) and vascular smooth muscle cells (αSMC; red) in aortic root isolated from *APOB*^{TG}*Apobec*$^{-/-}$*Ldlr*$^{+/-}$ mice treated with the LNA control or LNA 148a ($n = 9$ –10 per group). Quantification of CD68 and SMC positive area is shown in the bottom panel. Data are expressed as the average percentage of CD68-positive or SMC-positive signals per total lesion area; * $p < 0.05$, level of significance was determined using the Mann–Whitney test. Scale bars, 200 μm.

these results demonstrated that suppression of miR-148a results in increased macrophage cholesterol efflux and a reduced proinflammatory response.

Next, we assessed the impact of targeting miR-148a on the progression of atherosclerosis. To this end, *APOB*^{TG}*Apobec*$^{-/-}$*Ldlr*$^{+/-}$ mice were fed a Western diet for 22 weeks and injected with an LNA control or LNA miR-148a every 3 days for the last 10 weeks. Notably, vascular lesion areas were significantly reduced in the aortic roots and whole aorta of the mice injected with LNA 148a compared to those injected with the LNA control (Fig. 2A, B). We further characterized atherosclerotic plaques by analyzing markers of inflammation and lesion stability. Analysis of atheroma revealed decreased accumulation of macrophages, without affecting smooth muscle cell content in lesions in the LNA 148a treated mice (Fig. 2**C**). The results also revealed a significant increase in the thickness of the fibrous cap and a reduction in plaque necrosis in the mice injected with LNA 148a (Fig. 2**D**). Taken together, these findings highlight the therapeutic potential of inhibiting miR-148a in attenuating the progression of atherosclerosis and promoting plaque stabilization.

4. Discussion

The most salient finding of this study is that therapeutic silencing of miR-148a protects against atherosclerosis progression. Mechanistically, suppression of miR-148a reduced vascular inflammation and macrophage accumulation in aortic lesions, without significantly affecting circulating lipoproteins. Specifically, miR-148a inhibition attenuated macrophage inflammatory responses and polarized macrophages toward an M2-like phenotype, which resulted in more stable plaques, characterized by a thicker fibrous cap layer and smaller necrotic cores.

We and others previously reported that acute (1 −2 weeks) silencing of miR-148a in hypercholesterolemic mice (*Apoe*$^{-/-}$ and *Ldlr*$^{+/-}$*APOB*^{TG}) reduced plasma LDL-C levels and increased circulating HDL-C [35,37]. In this study, we found only modest effects of systemic inhibition of miR-148a on circulating lipoproteins in a different mouse model of hyperlipidemia (*APOB*^{TG}*Apobec*$^{-/-}$*Ldlr*$^{+/-}$ fed a Western diet) and treated with miR-148a LNA for a prolonged period (1 month). These results may be explained by the effect of the diet and genetic modifications in the mice used in the different studies on hepatic miR-148a levels. Additional studies in other animal models, such as mice with humanized livers or nonhuman primates that mimic human lipoprotein metabolism, are needed to determine the specific contribution of miR-148a silencing in reducing plasma LDL-C levels and its impact during atherogenesis.

In this study, although circulating LDL-C levels were not significantly reduced, miR-148a silencing markedly mitigated the progression of atherosclerosis in *APOB*^{TG}*Apobec*$^{-/-}$*Ldlr*$^{+/-}$ mice. Notably, miR-148a silencing attenuated the expression of proinflammatory cytokines, including interleukin-6 and TNF-α and promoted M2-like macrophage polarization. As reported previously, a macrophage phenotypic switch promotes tissue remodeling and repair through collagen formation and clearance of dying cells [48,49]. In agreement with the presence of such a switch, we observed that miR-148a silencing increased atherosclerotic plaque thickness and decreased necrosis, which correlated with a significant reduction in macrophage accumulation in lesions. Similar to our findings, several in vitro and in vivo studies reported that miR-148a expression influences murine and human macrophage polarization [41,50]. A previous study reported that overexpression of miR-148a suppresses colorectal cancer by inhibiting M2-like macrophage polarization and promoting the secretion of inflammatory cytokines associated with M1 polarization [51]. In addition to the regulation of cholesterol efflux and macrophage polarization, miR-148a controls macrophage proliferation, survival, and recruitment [41,50], which might contribute to chronic inflammation in atherosclerotic lesions. Further studies are required to determine how miR-148a regulation of macrophage proliferation and/or recruitment influences the progression of atherosclerosis.

The mechanism by which miR-148a influences macrophage activation and polarization remains poorly understood. Huang et al. [51] showed that miR-148a stimulates M1 polarization through PTEN/AKT-mediated activation of nuclear factor-κB signaling. Other research demonstrated that in addition to regulating macrophage activation, miR-148a facilitates macrophage differentiation from monocytes in response to granulocyte macrophage colony-stimulating factor and facilitates the differentiation of monocyte-derived dendritic cells [41]. Furthermore, as reported previously, miR-148a expression is regulated by Notch signaling and induced by PU.1, a key transcription factor that regulates gene expression during myeloid activation [41]. Collectively, our results and those of previous studies indicate that miR-148a plays a key role in regulating macrophage differentiation, polarization, and cholesterol metabolism, thus influencing the progression of atherosclerosis. Most importantly, our findings demonstrate that systemic suppression of miR-148a mitigates atherosclerosis progression.

Funding

This study was supported by grants from the National Institutes of Health (R35HL135820 to CF-H), American Heart Association (20TPA35490416 to CF-H; 17SDG33110002 to NR), Ministerio de Ciencia, Innovación y Universidades (PID2019-104367RB-100), and Agencia Estatal de Investigación (AEI/10.13039/501100011033) within the Subprograma Ramón y Cajal (RYC-201722879 to NR). CIBER de Diabetes y Enfermedades Metabólicas Asociadas (CIBERDEM) is a project of Instituto de Salud Carlos III. Institut de Recerca de l'Hospital de la Santa Creu i Sant Pau is accredited by the Generalitat de Catalunya as a Centre de Recerca de Catalunya (CERCA).

CRediT authorship contribution statement

Noemi Rotllan: Conceptualization, Methodology, Validation, Formal analysis, Investigation, Resources, Writing – review & editing, Funding aquisition. **Xinbo Zhang**: Methodology, Validation, Formal analysis. **Alberto Canfrán-Duque**: Methodology, Validation, Formal analysis. **Leigh Goedeke**: Resources, editing. **Raquel Griñán**: Methodology, Validation, Formal analysis. **Cristina Ramírez**: Methodology, Validation, Formal analysis. **Yajaira Suárez**: Writing – review & editing. **Carlos Fernández-Hernando**: Conceptualization, Methodology, Validation, Formal analysis, Investigation, Resources, Writing – original draft, Writing – review & editing.

Disclosures

C. Fernández-Hernando and L. Goedeke have a patent on the use of miR-148a inhibitors to treat dyslipidemia and atherosclerosis. The other authors report no conflicts of interest.

Conflict of interest statement

All the authors declare that they do not have financial/personal interest or belief that could affect their objectivity.

Data Availability

Data will be made available on request.

Appendix A. Supporting information

Supplementary data associated with this article can be found in the online version at doi:10.1016/j.biopha.2022.113419.

References

[1] V. Ambros, The functions of animal microRNAs, Nature 431 (2004) 350–355.

[2] B. Aryal, A.K. Singh, N. Rotllan, N. Price, C. Fernandez-Hernando, MicroRNAs and lipid metabolism, Curr. Opin. Lipido 28 (2017) 273–280.
[3] D.P. Bartel, MicroRNAs: genomics, biogenesis, mechanism, and function, Cell 116 (2004) 281–297.
[4] V. Rottiers, A.M. Naar, MicroRNAs in metabolism and metabolic disorders, Nat. Rev. Mol. Cell Biol. 13 (2012) 239–250.
[5] N.L. Price, L. Goedeke, Y. Suarez, C. Fernandez-Hernando, miR-33 in cardiometabolic diseases: lessons learned from novel animal models and approaches, EMBO Mol. Med 13 (2021), e12606.
[6] N.L. Price, V. Miguel, W. Ding, A.K. Singh, S. Malik, N. Rotllan, A. Moshnikova, J. Toczek, C. Zeiss, M.M. Sadeghi, N. Arias, A. Baldan, O.A. Andreev, D. Rodriguez-Puyol, R. Bahal, Y.K. Reshetnyak, Y. Suarez, C. Fernandez-Hernando, S. Lamas, Genetic deficiency or pharmacological inhibition of miR-33 protects from kidney fibrosis, JCI Insight (2019) 4.
[7] K.J. Rayner, F.J. Sheedy, C.C. Esau, F.N. Hussain, R.E. Temel, S. Parathath, J. M. van Gils, A.J. Rayner, A.N. Chang, Y. Suarez, C. Fernandez-Hernando, E. A. Fisher, K.J. Moore, Antagonism of miR-33 in mice promotes reverse cholesterol transport and regression of atherosclerosis, J. Clin. Invest 121 (2011) 2921–2931.
[8] N. Rotllan, C.M. Ramirez, B. Aryal, C.C. Esau, C. Fernandez-Hernando, Therapeutic silencing of microRNA-33 inhibits the progression of atherosclerosis in Ldlr-/- mice–brief report, Arterioscler. Thromb. Vasc. Biol. 33 (2013) 1973–1977.
[9] M. Sahraei, B. Chaube, Y. Liu, J. Sun, A. Kaplan, N.L. Price, W. Ding, S. Oyaghire, R. Garcia-Milian, S. Mehta, Y.K. Reshetnyak, R. Bahal, P. Fiorina, P.M. Glazer, D. L. Rimm, C. Fernandez-Hernando, Y. Suarez, Suppressing miR-21 activity in tumor-associated macrophages promotes an antitumor immune response, J. Clin. Invest 129 (2019) 5518–5536.
[10] C.K. Glass, J.L.Atherosclerosis Witztum, the road ahead, Cell 104 (2001) 503–516.
[11] L. Goedeke, C. Fernandez-Hernando, Regulation of cholesterol homeostasis, Cell Mol. Life Sci. 69 (2012) 915–930.
[12] E. Ikonen, Mechanisms for cellular cholesterol transport: defects and human disease, Physiol. Rev. 86 (2006) 1237–1261.
[13] I. Tabas, G. Garcia-Cardena, G.K. Owens, Recent insights into the cellular biology of atherosclerosis, J. Cell Biol. 209 (2015) 13–22.
[14] A.J. Lusis, Atherosclerosis, Nature 407 (2000) 233–241.
[15] X. Zhang, W.C. Sessa, C. Fernandez-Hernando, Endothelial transcytosis of lipoproteins in atherosclerosis, Front Cardiovasc Med 5 (2018) 130.
[16] J.L. Goldstein, S.K. Basu, G.Y. Brunschede, M.S. Brown, Release of low density lipoprotein from its cell surface receptor by sulfated glycosaminoglycans, Cell 7 (1976) 85–95.
[17] J.L. Goldstein, M.S. Brown, Regulation of the mevalonate pathway, Nature 343 (1990) 425–430.
[18] J.D. Horton, Y. Bashmakov, I. Shimomura, H. Shimano, Regulation of sterol regulatory element binding proteins in livers of fasted and refed mice, Proc. Natl. Acad. Sci. USA 95 (1998) 5987–5992.
[19] J.D. Horton, J.L. Goldstein, M.S. Brown, SREBPs: activators of the complete program of cholesterol and fatty acid synthesis in the liver, J. Clin. Invest 109 (2002) 1125–1131.
[20] P. Tontonoz, Transcriptional and posttranscriptional control of cholesterol homeostasis by liver X receptors, Cold Spring Harb. Symp. Quant. Biol. 76 (2011) 129–137.
[21] B. Wang, P. Tontonoz, Liver X receptors in lipid signalling and membrane homeostasis, Nat. Rev. Endocrinol. 14 (2018) 452–463.
[22] T. de Aguiar Vallim, E. Tarling, T. Kim, M. Civelek, A. Baldan, C. Esau, P. Edwards, MicroRNA-144 regulates hepatic ABCA1 and plasma HDL following activation of the nuclear receptor FXR, Circ. Res (2013).
[23] J. Kim, H. Yoon, C.M. Ramirez, S.M. Lee, H.S. Hoe, C. Fernandez-Hernando, MiR-106b impairs cholesterol efflux and increases Abeta levels by repressing ABCA1 expression, Exp. Neurol. 235 (2012) 476–483.
[24] J. Krutzfeldt, N. Rajewsky, R. Braich, K.G. Rajeev, T. Tuschl, M. Manoharan, M. Stoffel, Silencing of microRNAs in vivo with 'antagomirs', Nature 438 (2005) 685–689.
[25] C.M. Ramirez, A. Davalos, L. Goedeke, A.G. Salerno, N. Warrier, D. Cirera-Salinas, Y. Suarez, C. Fernandez-Hernando, MicroRNA-758 regulates cholesterol efflux through posttranscriptional repression of ATP-binding cassette transporter A1, Arterioscler. Thromb. Vasc. Biol. 31 (2011) 2707–2714.
[26] C.M. Ramirez, N. Rotllan, A.V. Vlassov, A. Davalos, M. Li, L. Goedeke, J.F. Aranda, D. Cirera-Salinas, E. Araldi, A. Salerno, A.C. Wanschel, J. Zavadil, A. Castrillo, K. Jungsu, Y. Suarez, C. Fernandez-Hernando, Control of Cholesterol Metabolism and Plasma HDL Levels by miRNA-144, Circ. Res (2013).
[27] J. Soh, J. Iqbal, J. Queiroz, C. Fernandez-Hernando, M.M. Hussain, MicroRNA-30c reduces hyperlipidemia and atherosclerosis in mice by decreasing lipid synthesis and lipoprotein secretion, Nat. Med 19 (2013) 892–900.
[28] K.C. Vickers, S.R. Landstreet, M.G. Levin, B.M. Shoucri, C.L. Toth, R.C. Taylor, B. T. Palmisano, F. Tabet, H.L. Cui, K.A. Rye, P. Sethupathy, A.T. Remaley, MicroRNA-223 coordinates cholesterol homeostasis, Proc. Natl. Acad. Sci. USA 111 (2014) 14518–14523.
[29] K.C. Vickers, B.M. Shoucri, M.G. Levin, H. Wu, D.S. Pearson, D. Osei-Hwedieh, F. S. Collins, A.T. Remaley, P. Sethupathy, MicroRNA-27b is a regulatory hub in lipid metabolism and is altered in dyslipidemia, Hepatology 57 (2013) 533–542.
[30] A. Davalos, L. Goedeke, P. Smibert, C.M. Ramirez, N.P. Warrier, U. Andreo, D. Cirera-Salinas, K. Rayner, U. Suresh, J.C. Pastor-Pareja, E. Esplugues, E. A. Fisher, L.O. Penalva, K.J. Moore, Y. Suarez, E.C. Lai, C. Fernandez-Hernando, miR-33a/b contribute to the regulation of fatty acid metabolism and insulin signaling, Proc. Natl. Acad. Sci. USA 108 (2011) 9232–9237.
[31] I. Gerin, L.A. Clerbaux, O. Haumont, N. Lanthier, A.K. Das, C.F. Burant, I. A. Leclercq, O.A. MacDougald, G.T. Bommer, Expression of miR-33 from an SREBP2 intron inhibits cholesterol export and fatty acid oxidation, J. Biol. Chem. 285 (2010) 33652–33661.
[32] T.J. Marquart, R.M. Allen, D.S. Ory, A. Baldan, miR-33 links SREBP-2 induction to repression of sterol transporters, Proc. Natl. Acad. Sci. USA 107 (2010) 12228–12232.
[33] S.H. Najafi-Shoushtari, F. Kristo, Y. Li, T. Shioda, D.E. Cohen, R.E. Gerszten, A. M. Naar, MicroRNA-33 and the SREBP host genes cooperate to control cholesterol homeostasis, Science 328 (2010) 1566–1569.
[34] K.J. Rayner, Y. Suarez, A. Davalos, S. Parathath, M.L. Fitzgerald, N. Tamehiro, E. A. Fisher, K.J. Moore, C. Fernandez-Hernando, MiR-33 contributes to the regulation of cholesterol homeostasis, Science 328 (2010) 1570–1573.
[35] L. Goedeke, N. Rotllan, A. Canfran-Duque, J.F. Aranda, C.M. Ramirez, E. Araldi, C. S. Lin, N.N. Anderson, A. Wagschal, R. de Cabo, J.D. Horton, M.A. Lasuncion, A. M. Naar, Y. Suarez, C. Fernandez-Hernando, MicroRNA-148a regulates LDL receptor and ABCA1 expression to control circulating lipoprotein levels, Nat. Med 21 (2015) 1280–1289.
[36] L. Goedeke, A. Wagschal, C. Fernandez-Hernando, A.M. Naar, miRNA regulation of LDL-cholesterol metabolism, Biochim Biophys. Acta 1861 (2016) 2047–2052.
[37] A. Wagschal, S.H. Najafi-Shoushtari, L. Wang, L. Goedeke, S. Sinha, A.S. deLemos, J.C. Black, C.M. Ramirez, Y. Li, R. Tewhey, I. Hatoum, N. Shah, Y. Lu, F. Kristo, N. Psychogios, V. Vrbanac, Y.C. Lu, T. Hla, R. de Cabo, J.S. Tsang, E. Schadt, P. C. Sabeti, S. Kathiresan, D.E. Cohen, J. Whetstine, R.T. Chung, C. Fernandez-Hernando, L.M. Kaplan, A. Bernards, R.E. Gerszten, A.M. Naar, Genome-wide identification of microRNAs regulating cholesterol and triglyceride homeostasis, Nat. Med 21 (2015) 1290–1297.
[38] R. Do, C.J. Willer, E.M. Schmidt, S. Sengupta, C. Gao, G.M. Peloso, S. Gustafsson, S. Kanoni, A. Ganna, J. Chen, M.L. Buchkovich, S. Mora, J.S. Beckmann, J.L. Bragg-Gresham, H.Y. Chang, A. Demirkan, H.M. Den Hertog, L.A. Donnelly, G.B. Ehret, T. Esko, M.F. Feitosa, T. Ferreira, K. Fischer, P. Fontanillas, R.M. Fraser, D. F. Freitag, D. Gurdasani, K. Heikkila, E. Hypponen, A. Isaacs, A.U. Jackson, A. Johansson, T. Johnson, M. Kaakinen, J. Kettunen, M.E. Kleber, X. Li, J. Luan, L. P. Lyytikainen, P.K. Magnusson, M. Mangino, E. Mihailov, M.E. Montasser, M. Muller-Nurasyid, I.M. Nolte, J.R. O'Connell, C.D. Palmer, M. Perola, A. K. Petersen, S. Sanna, R. Saxena, S.K. Service, S. Shah, D. Shungin, C. Sidore, C. Song, R.J. Strawbridge, I. Surakka, T. Tanaka, T.M. Teslovich, G. Thorleifsson, E. G. Van den Herik, B.F. Voight, K.A. Volcik, L.L. Waite, A. Wong, Y. Wu, W. Zhang, D. Absher, G. Asiki, I. Barroso, L.F. Been, J.L. Bolton, L.L. Bonnycastle, P. Brambilla, M.S. Burnett, G. Cesana, M. Dimitriou, A.S. Doney, A. Doring, P. Elliott, S.E. Epstein, G.I. Eyjolfsson, B. Gigante, M.O. Goodarzi, H. Grallert, M. L. Gravito, C.J. Groves, G. Hallmans, A.L. Hartikainen, C. Hayward, D. Hernandez, A.A. Hicks, H. Holm, Y.J. Hung, T. Illig, M.R. Jones, P. Kaleebu, J.J. Kastelein, K. T. Khaw, E. Kim, N. Klopp, P. Komulainen, M. Kumari, C. Langenberg, T. Lehtimaki, S.Y. Lin, J. Lindstrom, R.J. Loos, F. Mach, W.L. McArdle, C. Meisinger, B.D. Mitchell, G. Muller, R. Nagaraja, N. Narisu, T.V. Nieminen, R. N. Nsubuga, I. Olafsson, K.K. Ong, A. Palotie, T. Papamarkou, C. Pomilla, A. Pouta, D.J. Rader, M.P. Reilly, P.M. Ridker, F. Rivadeneira, I. Rudan, A. Ruokonen, N. Samani, H. Scharnagl, J. Seeley, K. Silander, A. Stancakova, K. Stirrups, A. J. Swift, L. Tiret, A.G. Uitterlinden, L.J. van Pelt, S. Vedantam, N. Wainwright, C. Wijmenga, S.H. Wild, G. Willemsen, T. Wilsgaard, J.F. Wilson, E.H. Young, J. H. Zhao, L.S. Adair, D. Arveiler, T.L. Assimes, S. Bandinelli, F. Bennett, M. Bochud, B.O. Boehm, D.I. Boomsma, I.B. Borecki, S.R. Bornstein, P. Bovet, M. Burnier, H. Campbell, A. Chakravarti, J.C. Chambers, Y.D. Chen, F.S. Collins, R.S. Cooper, J. Danesh, G. Dedoussis, U. de Faire, A.B. Feranil, J. Ferrieres, L. Ferrucci, N. B. Freimer, C. Gieger, L.C. Groop, V. Gudnason, U. Gyllensten, A. Hamsten, T. B. Harris, A. Hingorani, J.N. Hirschhorn, A. Hofman, G.K. Hovingh, C.A. Hsiung, S. E. Humphries, S.C. Hunt, K. Hveem, C. Iribarren, M.R. Jarvelin, A. Jula, M. Kahonen, J. Kaprio, A. Kesaniemi, M. Kivimaki, J.S. Kooner, P.J. Koudstaal, R. M. Krauss, D. Kuh, J. Kuusisto, K.O. Kyvik, M. Laakso, T.A. Lakka, L. Lind, C. M. Lindgren, N.G. Martin, W. Marz, M.I. McCarthy, C.A. McKenzie, P. Meneton, A. Metspalu, L. Moilanen, A.D. Morris, P.B. Munroe, I. Njolstad, N.L. Pedersen, C. Power, P.P. Pramstaller, J.F. Price, B.M. Psaty, T. Quertermous, R. Rauramaa, D. Saleheen, V. Salomaa, D.K. Sanghera, J. Saramies, P.E. Schwarz, W.H. Sheu, A. R. Shuldiner, A. Siegbahn, T.D. Spector, K. Stefansson, D.P. Strachan, B.O. Tayo, E. Tremoli, J. Tuomilehto, M. Uusitupa, C.M. van Duijn, P. Vollenweider, L. Wallentin, N.J. Wareham, J.B. Whitfield, B.H. Wolffenbuttel, D. Altshuler, J. M. Ordovas, E. Boerwinkle, C.N. Palmer, U. Thorsteinsdottir, D.I. Chasman, J. I. Rotter, P.W. Franks, S. Ripatti, L.A. Cupples, M.S. Sandhu, S.S. Rich, M. Boehnke, P. Deloukas, K.L. Mohlke, E. Ingelsson, G.R. Abecasis, M.J. Daly, B.M. Neale, S. Kathiresan, Common variants associated with plasma triglycerides and risk for coronary artery disease, Nat. Genet 45 (2013) 1345–1352.
[39] C.J. Willer, E.M. Schmidt, S. Sengupta, G.M. Peloso, S. Gustafsson, S. Kanoni, A. Ganna, J. Chen, M.L. Buchkovich, S. Mora, J.S. Beckmann, J.L. Bragg-Gresham, H.Y. Chang, A. Demirkan, H.M. Den Hertog, R. Do, L.A. Donnelly, G.B. Ehret, T. Esko, M.F. Feitosa, T. Ferreira, K. Fischer, P. Fontanillas, R.M. Fraser, D. F. Freitag, D. Gurdasani, K. Heikkila, E. Hypponen, A. Isaacs, A.U. Jackson, A. Johansson, T. Johnson, M. Kaakinen, J. Kettunen, M.E. Kleber, X. Li, J. Luan, L. P. Lyytikainen, P.K.E. Magnusson, M. Mangino, E. Mihailov, M.E. Montasser, M. Muller-Nurasyid, I.M. Nolte, J.R. O'Connell, C.D. Palmer, M. Perola, A. K. Petersen, S. Sanna, R. Saxena, S.K. Service, S. Shah, D. Shungin, C. Sidore, C. Song, R.J. Strawbridge, I. Surakka, T. Tanaka, T.M. Teslovich, G. Thorleifsson, E. G. Van den Herik, B.F. Voight, K.A. Volcik, L.L. Waite, A. Wong, Y. Wu, W. Zhang, D. Absher, G. Asiki, I. Barroso, L.F. Been, J.L. Bolton, L.L. Bonnycastle, P. Brambilla, M.S. Burnett, G. Cesana, M. Dimitriou, A.S.F. Doney, A. Doring, P. Elliott, S.E. Epstein, G. Ingi Eyjolfsson, B. Gigante, M.O. Goodarzi, H. Grallert, M. L. Gravito, C.J. Groves, G. Hallmans, A.L. Hartikainen, C. Hayward, D. Hernandez, A.A. Hicks, H. Holm, Y.J. Hung, T. Illig, M.R. Jones, P. Kaleebu, J.J.P. Kastelein, K.

T. Khaw, E. Kim, N. Klopp, P. Komulainen, M. Kumari, C. Langenberg, T. Lehtimaki, S.Y. Lin, J. Lindstrom, R.J.F. Loos, F. Mach, W.L. McArdle, C. Meisinger, B.D. Mitchell, G. Muller, R. Nagaraja, N. Narisu, T.V.M. Nieminen, R. N. Nsubuga, I. Olafsson, K.K. Ong, A. Palotie, T. Papamarkou, C. Pomilla, A. Pouta, D.J. Rader, M.P. Reilly, P.M. Ridker, F. Rivadeneira, I. Rudan, A. Ruokonen, N. Samani, H. Scharnagl, J. Seeley, K. Silander, A. Stancakova, K. Stirrups, A. J. Swift, L. Tiret, A.G. Uitterlinden, L.J. van Pelt, S. Vedantam, N. Wainwright, C. Wijmenga, S.H. Wild, G. Willemsen, T. Wilsgaard, J.F. Wilson, E.H. Young, J. H. Zhao, L.S. Adair, D. Arveiler, T.L. Assimes, S. Bandinelli, F. Bennett, M. Bochud, B.O. Boehm, D.I. Boomsma, I.B. Borecki, S.R. Bornstein, P. Bovet, M. Burnier, H. Campbell, A. Chakravarti, J.C. Chambers, Y.I. Chen, F.S. Collins, R.S. Cooper, J. Danesh, G. Dedoussis, U. de Faire, A.B. Feranil, J. Ferrieres, L. Ferrucci, N. B. Freimer, C. Gieger, L.C. Groop, V. Gudnason, U. Gyllensten, A. Hamsten, T. B. Harris, A. Hingorani, J.N. Hirschhorn, A. Hofman, G.K. Hovingh, C.A. Hsiung, S. E. Humphries, S.C. Hunt, K. Hveem, C. Iribarren, M.R. Jarvelin, A. Jula, M. Kahonen, J. Kaprio, A. Kesaniemi, M. Kivimaki, J.S. Kooner, P.J. Koudstaal, R. M. Krauss, D. Kuh, J. Kuusisto, K.O. Kyvik, M. Laakso, T.A. Lakka, L. Lind, C. M. Lindgren, N.G. Martin, W. Marz, M.I. McCarthy, C.A. McKenzie, P. Meneton, A. Metspalu, L. Moilanen, A.D. Morris, P.B. Munroe, I. Njolstad, N.L. Pedersen, C. Power, P.P. Pramstaller, J.F. Price, B.M. Psaty, T. Quertermous, R. Rauramaa, D. Saleheen, V. Salomaa, D.K. Sanghera, J. Saramies, P.E.H. Schwarz, W.H. Sheu, A.R. Shuldiner, A. Siegbahn, T.D. Spector, K. Stefansson, D.P. Strachan, B.O. Tayo, E. Tremoli, J. Tuomilehto, M. Uusitupa, C.M. van Duijn, P. Vollenweider, L. Wallentin, N.J. Wareham, J.B. Whitfield, B.H.R. Wolffenbuttel, J.M. Ordovas, E. Boerwinkle, C.N.A. Palmer, U. Thorsteinsdottir, D.I. Chasman, J.I. Rotter, P. W. Franks, S. Ripatti, L.A. Cupples, M.S. Sandhu, S.S. Rich, M. Boehnke, P. Deloukas, S. Kathiresan, K.L. Mohlke, E. Ingelsson, G.R. Abecasis, and Global Lipids Genetics C. Discovery and refinement of loci associated with lipid levels, Nat. Genet. 45 (2013) 1274–1283.

[40] X. Bai, J. Li, L. Li, M. Liu, Y. Liu, M. Cao, K. Tao, S. Xie, D. Hu, Extracellular vesicles from adipose tissue-derived stem cells affect notch-miR148a-3p Axis to regulate polarization of macrophages and alleviate sepsis in mice, Front Immunol. 11 (2020) 1391.

[41] F. Huang, J.L. Zhao, L. Wang, C.C. Gao, S.Q. Liang, D.J. An, J. Bai, Y. Chen, H. Han, H.Y. Qin, miR-148a-3p mediates notch signaling to promote the differentiation and m1 activation of macrophages, Front Immunol. 8 (2017) 1327.

[42] X. Liu, Z. Zhan, L. Xu, F. Ma, D. Li, Z. Guo, N. Li, X. Cao, MicroRNA-148/152 impair innate response and antigen presentation of TLR-triggered dendritic cells by targeting CaMKIIalpha, J. Immunol. 185 (2010) 7244–7251.

[43] Y. Chen, Y.X. Song, Z.N. Wang, The microRNA-148/152 family: multi-faceted players, Mol. Cancer 12 (2013) 43.

[44] L. Shang, A. Quan, H. Sun, Y. Xu, G. Sun, P. Cao, MicroRNA-148a-3p promotes survival and migration of endothelial cells isolated from Apoe deficient mice through restricting circular RNA 0003575, Gene 711 (2019), 143948.

[45] T.A. Seimon, Y. Wang, S. Han, T. Senokuchi, D.M. Schrijvers, G. Kuriakose, A. R. Tall, I.A. Tabas, Macrophage deficiency of p38alpha MAPK promotes apoptosis and plaque necrosis in advanced atherosclerotic lesions in mice, J. Clin. Invest 119 (2009) 886–898.

[46] L. Goedeke, A. Salerno, C.M. Ramirez, L. Guo, R.M. Allen, X. Yin, S.R. Langley, C. Esau, A. Wanschel, E.A. Fisher, Y. Suarez, A. Baldan, M. Mayr, C. Fernandez-Hernando, Long-term therapeutic silencing of miR-33 increases circulating triglyceride levels and hepatic lipid accumulation in mice, EMBO Mol. Med 6 (2014) 1133–1141.

[47] C.M. Ramirez, A. Davalos, L. Goedeke, A.G. Salerno, N. Warrier, D. Cirera-Salinas, Y. Suarez, C. Fernandez-Hernando, MicroRNA-758 regulates cholesterol efflux through posttranscriptional repression of ATP-binding cassette transporter A1, Arterioscler., Thromb., Vasc. Biol. 31 (2011) 2707–2714.

[48] G.J. Koelwyn, E.M. Corr, E. Erbay, K.J. Moore, Regulation of macrophage immunometabolism in atherosclerosis, Nat. Immunol. 19 (2018) 526–537.

[49] K.J. Moore, I. Tabas, Macrophages in the pathogenesis of atherosclerosis, Cell 145 (2011) 341–355.

[50] D. Ma, Y. Zhang, G. Chen, J. Yan, miR-148a affects polarization of THP-1-derived macrophages and reduces recruitment of tumor-associated macrophages via targeting SIRPalpha, Cancer Manag. Res. 12 (2020) 8067–8077.

[51] Y. Zhu, L. Gu, Y. Li, X. Lin, H. Shen, K. Cui, L. Chen, F. Zhou, Q. Zhao, J. Zhang, B. Zhong, E. Prochownik, Y. Li, miR-148a inhibits colitis and colitis-associated tumorigenesis in mice, Cell Death Differ. 24 (2017) 2199–2209.